Supporting Information

of

Reshaping Prostate Tumor Microenvironment To Suppress Metastasis *via* Cancer-Associated Fibroblast Inactivation with Peptide-Assembly-Based Nanosystem

Jiayan Lang,†§#∇ Xiao Zhao,†# ∇ Yingqiu Qi,†Ψ Yinlong Zhang,†∇ Xuexiang Han,†∇ Yanping Ding,†∇ Jiajing Guan,† Tianjiao Ji,†∇ Ying Zhao,†∇* Guangjun Nie,†∇**

† CAS Key Laboratory for Biomedical Effects of Nanomaterials & Nanosafety, CAS Center for Excellence in Nanoscience, National Center for Nanoscience and Technology, Beijing 100190, China

§ Sino-Danish Center for Education and Research/ Sino-Danish College of UCAS, Beijing, 100190, China

Ψ School of Basic Medical Sciences, Zhengzhou University, Henan 450001, China

∇ Center of Materials Science and Optoelectronics Engineering, University of Chinese Academy of Sciences, Beijing 100049, China

***Address correspondence to:**

Tianjiao Ji, Ying Zhao and Guangjun Nie

Email: jitj@nanoctr.cn, zhaoying@nanoctr.cn, niegj@nanoctr.cn

Supporting Tables and Figures

Table S1. Particle size, polydispersity index (PDI) and zeta potential of optimized nanoparticles.

Groups	Particle size (nm)	PDI	Zeta potential (mV)
PNP	31.2 ± 1.5	0.125	42.9 ± 1.1
PNP/siRNA	85.5 ± 4.3	0.195	43.2 ± 3.5
PNP/siRNA/mAb	102.4 ± 4.5	0.268	-13.2 ± 1.4
PNP/siRNA/IgG	106.2 ± 5.3	0.279	-13.1 ± 1.7

Samples were prepared in 10 mM HEPES buffer (pH 7.4) and data were collected by DLS measurements. The data are presented as the mean ± SD (n = 3).

Table S2 Expression changes of cytokines in CAFs after treated with PNP/si*CXCL12*/mAb.

Function	Name	% change
Positive regulation of cell proliferation	LIF	-44.8
	IL-6	-56.8
	FGF7	-77.0
	MCP-1/CCL2	-61.2
	ENA-78/CXCL5	-68.0
	FGF9	-73.9
	Angiogenin	-42.2
	VEGF	-82.2
	EGF	-45.9
	TGF-β1	-85.0
	Flt-3 Ligand	-69.3
	IP-10/CXCL10	-73.3
Regulation of endothelial cell proliferation	MCP-1/CCL2	-61.2
	Angiogenin	-42.2
	VEGFA	-82.2
Positive regulation of cell migration	IL-6	-56.8
	VEGF	-82.2
	SDF-1/CXCL12	-93.3
	TGF-β1	-85.0
	IP-10/CXCL10	-73.3
Positive regulation of blood vessel endothelial cell migration	VEGFA	-82.2
	TGF-β1	-85.0

Significant enriched pathways for genes upregulated of CAFs in PNP/si*CXCL12*/mAb group versus PNP/si*N.C.*/mAb group. The decreased cytokines (the change of which was more than 40%) secreted by PNP/si*CXCL12*/mAb treated CAF was subjected to pathway analysis using DAVID web software based on Gene Ontology (GO) and

KEGG（KyotoEncyclopedia of Genes and Genomes) database.

Change (%) = ($PD_{siN.C.}$- $PD_{siCXCL12}$)/ $PD_{siN.C.}$×100%

LIF: leukemia inhibitory factor, IL6: interleukin 6, FGF7: fibroblast growth factor 7, MCP-1: monocyte chemoattractant protein-1, ENG-78: epithelial neutrophil activating peptide 78, VEGF: vascular endothelial growth factor, EGF: epidermal growth factor, TGF-β: transforming growth factor-β, Flt-3 Ligand: Fms-related tyrosine kinase 3 ligand, IP-10: Interferon gamma-induced protein 10.

Table S3. Expression changes of angiogenesis-related cytokines secreted by CAFs after treated with PNP/si*CXCL12*/mAb.

	Name	% change	Angiogenesis
Decrease factors	VEGF	-79.28	pro-
	FGF-4	-76.9	pro-
	FGF acidic	-58.4	pro-
	FGF-7	-47.6	pro-
	FGF basic	-41.1	pro-
	EGF	-72.1	pro-
	VEGF	-41.2	pro-
	Leptin	-71.0	pro-
	Amphiregulin	-49.7	pro-
	Angiogenin	-41.5	pro-
	PF4	-57.6	anti-
	Angiostatin	-47.9	anti-
	MCP-1	-82.7	pro-
Increased factors	Thrombospondin-2	75.1	anti-
	Serpin B5	69.9	anti-

The change of whose were more than 40% are listed.

Change (%) = $(PD_{siN.C.} - PD_{siCXCL12})/ PD_{siN.C.} \times 100\%$

Pro-: pro-angiogenesis factor; Anti-: anti-angiogenesis factor

FGF: fibroblast growth factor, EGF: epidermal growth factor, VEGF: vascular endothelial growth factor, PF4: platelet factor 4, MCP-1: monocyte chemoattractant protein-1

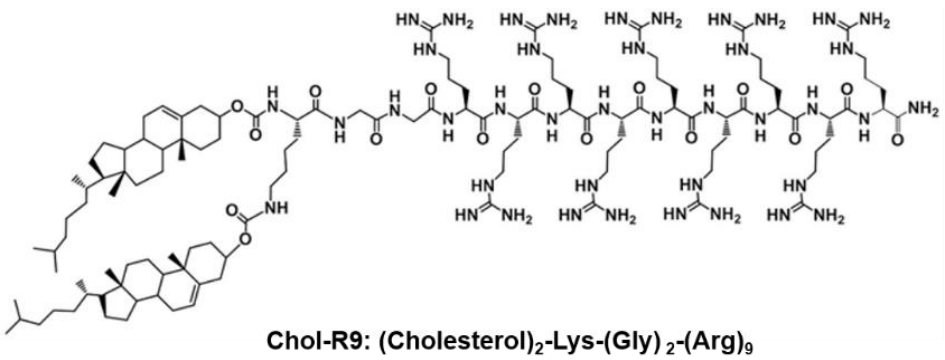

Figure S1. The molecular structure and sequences of the CPPs-based amphiphilic peptide, Chol-R9.

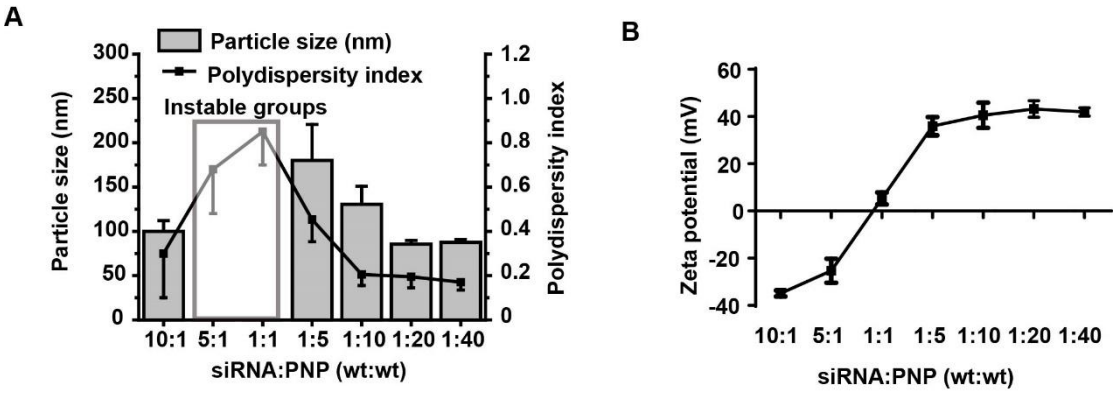

Figure S2. Characterization of the PNP/siRNA complexes with different weight ratio of siRNA and peptide nanoparticles (PNP). (A) Particle size and PDI of PNP/siRNA complexes with different ratios of siRNA and PNP. The groups in gray frame are instable. Data are shown as the mean ± SD (n = 3). (B) The zeta potential of PNP/siRNA complexes with different ratios of siRNA and PNP. Data are shown as the mean ± SD (n = 3).

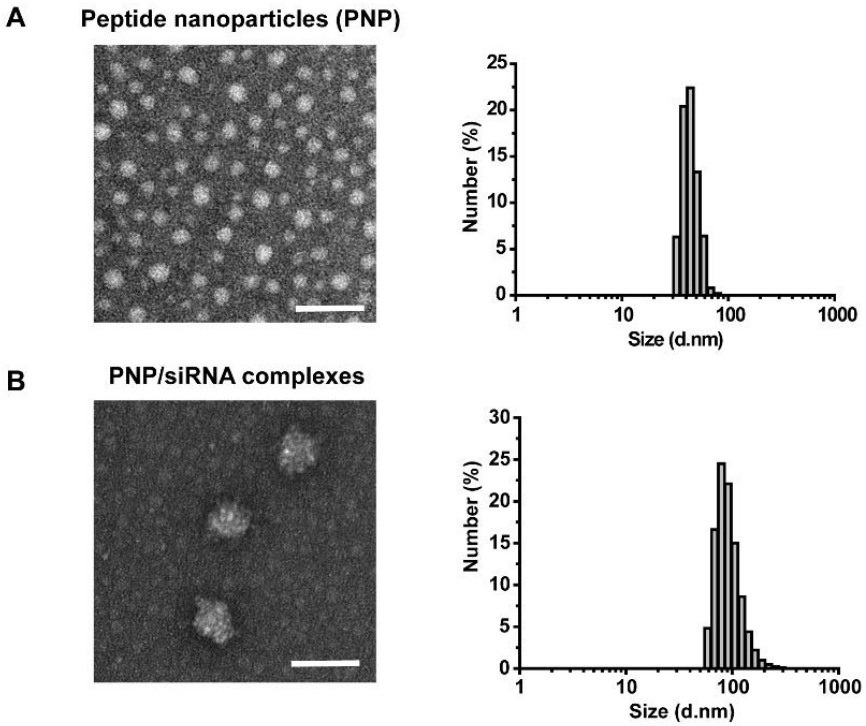

Figure S3. Morphologies and size distribution of Chole-R9 peptide nanoparticles (PNP) (A) and optimized PNP/siRNA complexes (B) detected by TEM (left) and DLS (right). The weight ratio of PNP to siRNA was 1:20. Scale bar: 100 nm. The PDI of PNP was 0.125; the PDI of PNP/siRNA complexes was 0.195.

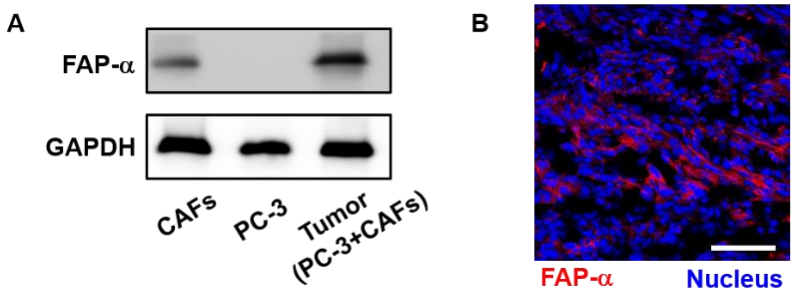

Figure S4. FAP-α expression in cells and tumor tissues. (A) FAP-α protein expression in CAFs, PC-3 cells, orthotopic prostate tumor tissue detected by western blot. (B) Immunofluorescence (IF) staining of FAP-α in CAFs and PC-3 cells co-implanted orthotopic prostate tumor tissue. Red: FAP-α; blue: Hoechst 33342, nucleus. Scale bar, 50 μm.

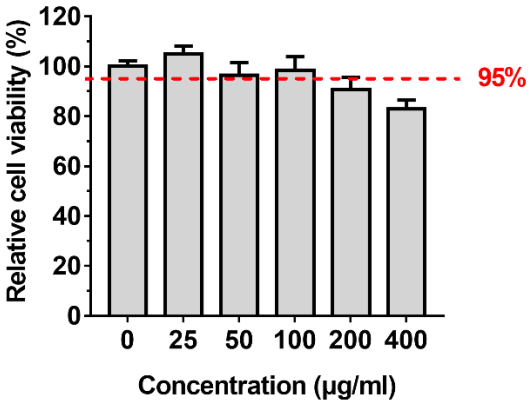

Figure S5. Cytotoxicity of PNP/si*N.C.*/mAb against CAFs at different PNP concentrations. si*N.C.* is negative control that has no significant sequence similarity to mouse and human gene sequences. The ratio of siRNA:PNP was 1:20 in PNP/si*N.C.*/mAb group. Data are shown as the mean ± SD (n = 5).

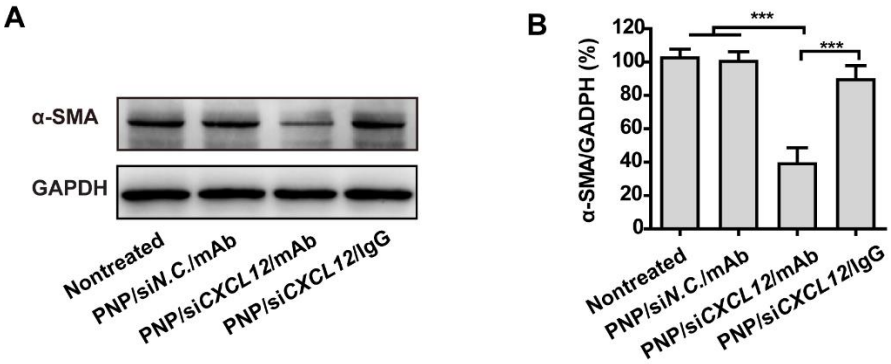

Figure S6. Western blot analysis of α-SMA expression in CAFs after different formulation treatment. (A) Western blot images of α-SMA expression in CAFs. B) Normalized protein expression levels of α-SMA in CAFs from western blot results (analyzed by ImageJ software). Data are shown as the mean ± SD (n = 3). ***$p < 0.001$.

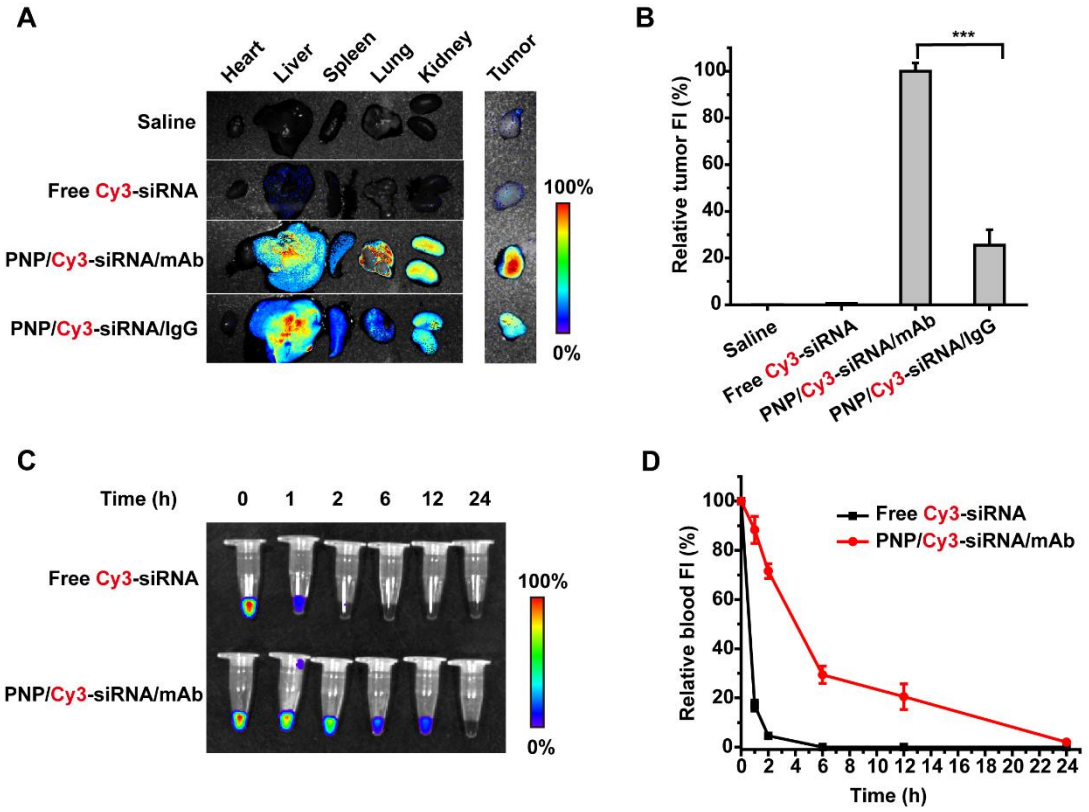

Figure S7. *In vivo* targeting and the blood clearance rate. (A) *Ex vivo* imaging of major organs (heart, liver, spleen, lung, kidney and tumor) detected by IVIS. Before imaging, Balb/c nude mice with orthotopic xenografts (PC-3 + CAFs) were respectively *i.v.* injected with saline, free Cy3-siRNA, PNP/Cy3-siRNA/mAb or PNP/Cy3-siRNA/IgG. (B) Quantitative analysis of relative fluorescence intensity (FI) of tumors in each group. Data are shown as the mean ± SD (n = 3). ***$p < 0.001$. (C, D) Blood clearance rate of siRNA and PNP/siRNA/mAb. Balb/c mice were intravenously injected free Cy3-siRNA and PNP/Cy3-siRNA/mAb. At different time points, blood was collected and imaged by using *in vivo* imaging system (C). Relative fluorescence intensity (FI) was calculated and quantified (D). Data are shown as the mean ± SD (n = 3), ***$p < 0.001$.

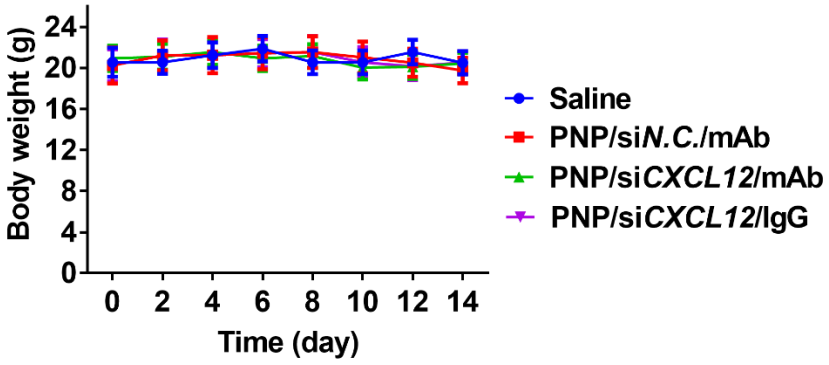

Figure S8. Body weight of mice during the treatment with each formulation.

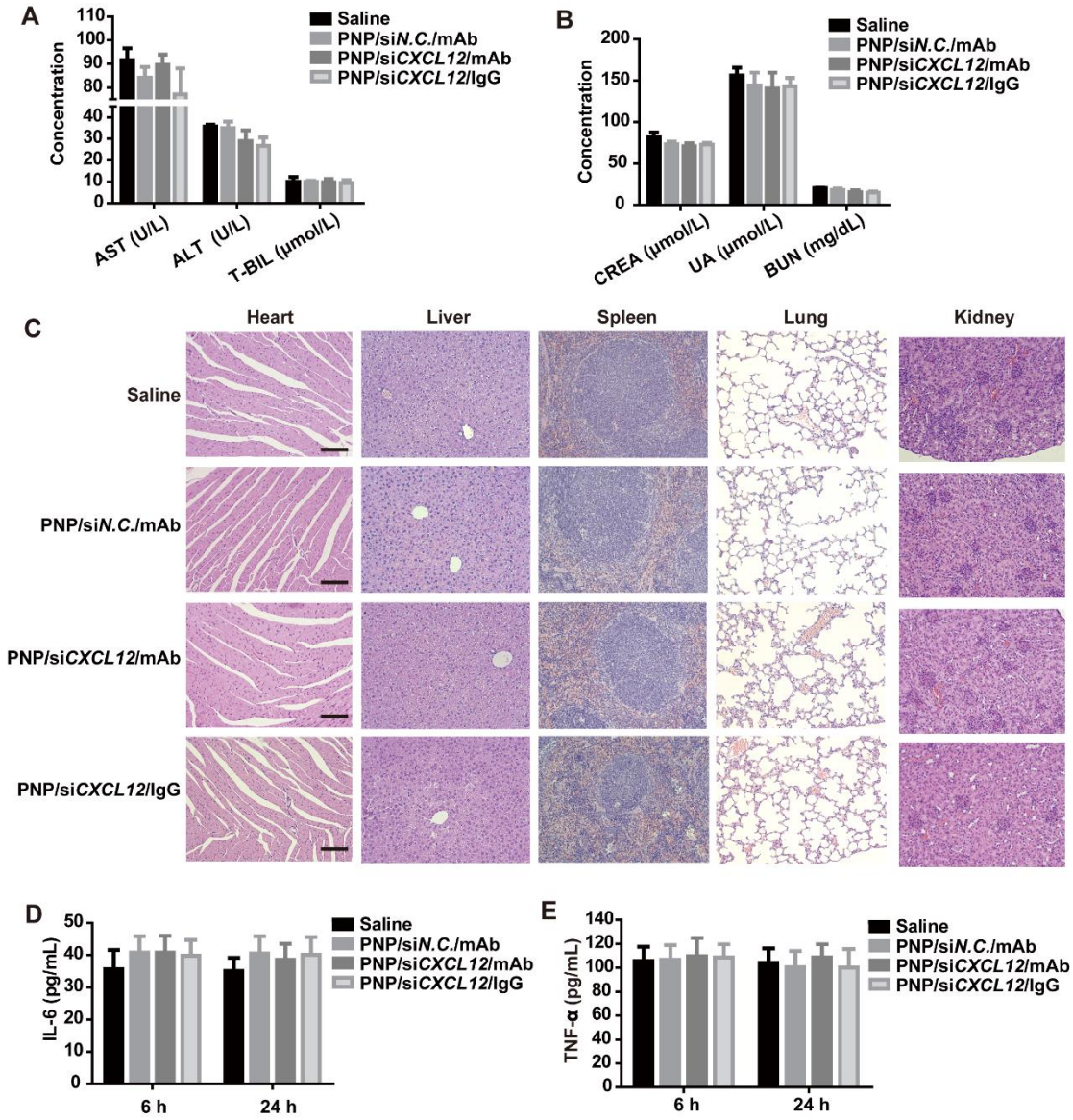

Figure S9. Bio-safety evaluation of formulations. Serum levels of biochemical indicators of liver (A) and kidney (B) damage in mice after six treatments of saline or various formulations. ALT, alanine aminotransferase; AST, aspartate transaminase; TBIL, total value bilirubin; CREA, creatinine; UA, uric acid; BUN, Blood urea nitrogen. Data are shown as mean ± SD (n = 4). (C) H&E staining slices of major organs (heart, liver, Spleen, lung, kidney). Scale bar, 100 μm. (D, E) Immune response of PNP/siRNA/mAb in Balb/c mice at 6 h and 24 h post-treatment. Interleukin-6 (IL-6) and tumor necrosis factor-α (TNF-α) in serum were measured by ELISA assay (n = 4).